

Five-body calculation of resonance and scattering states of pentaquark system

E. Hiyama^a, M. Kamimura^b, A. Hosaka^c, H. Toki^c and M. Yahiro^b

^a*Department of Physics, Nara Women's University, Nara 630-8506, Japan*

^b*Department of Physics, Kyushu University, Fukuoka 812-8581, Japan and*

^c*Research Center for Nuclear Physics (RCNP), Osaka University, Ibaraki, 567-0047, Japan*

Scattering problem of the $uudd\bar{s}$ system, in the standard non-relativistic quark model of Isgur-Karl, is solved for the first time, by treating the large five-body model space including the NK scattering channel accurately with the Gaussian expansion method and the Kohn-type coupled-channel variational method. The two-body interaction that reproduces observed properties of ordinary baryons and mesons is applied to the pentaquark system with no additional adjustable parameter. The five-body wave function calculated has the correct asymptotic form in its the scattering-channel component and describes qq and $q\bar{q}$ correlations properly. The NK scattering phase shift calculated shows no resonance in the energy region of the reported pentaquark $\Theta^+(1540)$, that is, at 0 – 500 MeV above the NK threshold (1.4 – 1.9 GeV in mass). The phase shift does show two resonances just above 500 MeV: a broad $\frac{1}{2}^+$ resonance with a width of $\Gamma \sim 110$ MeV located at ~ 520 MeV (~ 2.0 GeV in mass) and a sharp $\frac{1}{2}^-$ resonance with $\Gamma = 0.12$ MeV at 540 MeV. Properties of these states are discussed.

I. INTRODUCTION

The observation of a signal of a narrow resonance at ~ 1540 MeV with $S = +1$ by the LEPs group [1, 2], now called $\Theta^+(1540)$, triggered a lot of theoretical works on multi-quark systems [3], although further experimental reexamination is still needed to establish the state. The question whether the multi-quark baryon $\Theta^+(1540)$ really exists or not is then one of current issues in hadron physics. In order to answer the question theoretically, one has to nonperturbatively evaluate the mass and the decay width of $\Theta^+(1540)$, namely of the $uudd\bar{s}$ resonance. All nonperturbative analyses made so far, however, did not impose any proper boundary condition to the NK scattering component of the pentaquark state. At the present stage, the non-relativistic quark model provides a nonperturbative framework which makes it possible to impose a proper boundary condition to the NK scattering component.

In this paper, we take the standard quark model of Isgur-Karl [4, 5]. The Hamiltonian consists of the confining potential of harmonic oscillator type and the color-magnetic spin-spin interaction. As shown later, the Hamiltonian satisfactorily reproduces observed properties of ordinary baryons and mesons. The same Hamiltonian is applied to the pentaquark with no adjustable parameter.

Resonant and non-resonant states of the $uudd\bar{s}$ system are nonperturbatively derived with the Kohn-type coupled-channel variational method [6] in which a proper boundary condition is imposed to the NK scattering channel and the total antisymmetrization between quarks is explicitly taken into account. Reliability of the method for scattering problem between composite particles was shown by one of the authors (M.K.) [6], and actually it was already applied to $qqq - qqq$ scattering [7].

The coupled-channel variational method is accurate, only when the five-body dynamics in the interaction region is solved precisely. As such a method, we use the Gaussian expansion method (GEM) [8]. GEM is one of

the most reliable few-body methods proposed by two of the present authors (E.H. and M.K.) and their collaborators. The method was successfully applied to various types of three- and four-body systems [8]. For instance, the mass of antiproton [9] was evaluated precisely, i.e. with eight-digit accuracy, by comparing the three-body GEM calculation [10] with CERN's high-resolution laser spectroscopy data [11] on highly excited three-body resonance states of antiprotonic helium atom ($^4\text{He}^{++} + \bar{p} + e^-$).

The five-body model space considered here consists of two parts: the asymptotic-region part describing NK scattering and the interaction-region part. In this paper, the interaction-region part is accurately described as a superposition of an enormous number of L^2 -type basis functions. As internal coordinates of the five-body system, we take five types of Jacobi-coordinate sets shown in Fig. 1. Advantages in using several rearrangement Jacobi-coordinate sets simultaneously are reviewed in [8]. This setting can accommodate a wide (practically sufficient) model space, as shown later. Sets $c = 4$ and 5 of Fig. 1 contain internal coordinates of two qq pairs, so these sets can treat qq correlations properly with the basis functions of the internal coordinates. Similarly, sets $c = 1 - 3$ are convenient for handling qq and $q\bar{q}$ correlations. In general, the two-body correlation in the color-singlet $(q\bar{q})_1$ pair is twice as strong as that in the color-antitriplet $(qq)_3$ pair due to the $SU(3)$ color operator. Sets 1 – 3 contain two $(q\bar{q})_1$ pairs, while sets 4 and 5 do a $(q\bar{q})_1$ pair and a $(qq)_3$ pair. Thus, use of sets 1 – 3 is indispensable. In principle, four more Jacobi-coordinate sets are possible, but these are much less important since they contain only one qq or $q\bar{q}$ pair.

The five Jacobi-coordinate sets can be classified into $c = 1 - 3$ and $c = 4, 5$. We call the latter two sets ($c = 4, 5$) the "connected" configurations in the sense that they contain no color-singlet cluster; while we call the former sets ($c = 1 - 3$) the "molecular" ones as they are composed of color-singlet clusters. The explicit definitions of these configurations are shown later. Ob-

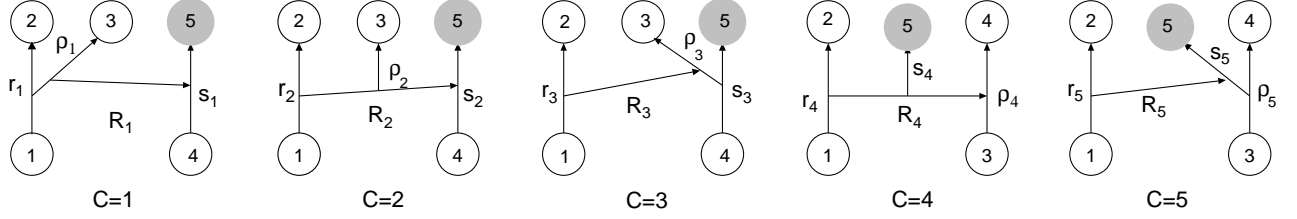


FIG. 1: Five sets of Jacobi coordinates among five quarks. Four u, d quarks, labeled by particle 1–4, are to be antisymmetrized, while particle 5 stands for \bar{s} quark. Sets $c = 4, 5$ contain two qq correlations, while sets $c = 1 - 3$ do both qq and $q\bar{q}$ correlations. Sets $c = 4, 5$ describe molecular configurations and sets $c = 1 - 3$ does connected ones, as shown in the text. The NK scattering channel is treated with $c = 1$.

viously, the NK scattering component, described with $c = 1$, is molecular since it contains color-singlet qqq and $q\bar{q}$ clusters.

We consider three spin-parity states, $J^\pi = \frac{1}{2}^-$ and $J^\pi = \frac{1}{2}^+$ and $\frac{3}{2}^+$, with a common isospin $T = 0$. In this model Hamiltonian, the $J^\pi = \frac{1}{2}^+$ and $\frac{3}{2}^+$ states are degenerate in the absence of spin-orbit forces between quarks. (Such a spin-orbit interaction leads to mass splitting between $J^\pi = \frac{1}{2}^+$ and $\frac{3}{2}^+$ and influence on their phase shift Ref. [15, 16].). Thus, our analysis is focused on the $J^\pi = \frac{1}{2}^+$ state. As shown later, the calculated phase shift exhibits no resonance when only the NK channel is taken and then no excitation of N and K is taken into account. Therefore, of importance is whether the five-body dynamics in the interaction region can generate any resonance in the intermediate stage of scattering, particularly in the energy region of $\Theta^+(1540)$. Furthermore, if a resonance appears, of interest is whether it has the connected configuration or the molecular one.

II. MODEL HAMILTONIAN

Hamiltonian of the standard non-relativistic quark model of Isgur-Karl [4, 5] is

$$H = \sum_i \left(m_i + \frac{\mathbf{p}_i^2}{2m_i} \right) - T_G + V_{\text{Conf}} + V_{\text{CM}}, \quad (2.1)$$

where m_i and \mathbf{p}_i are the mass and momentum of i th quark and T_G is the kinetic energy of the center-of-mass system. In what follows, u and d quarks are labeled by $i = 1 - 4$, and \bar{s} by $i = 5$. The confining potential V_{Conf} is of harmonic oscillator type:

$$V_{\text{Conf}} = - \sum_{i < j} \sum_{\alpha=1}^8 \frac{\lambda_i^\alpha}{2} \frac{\lambda_j^\alpha}{2} \left[\frac{k}{2} (\mathbf{x}_i - \mathbf{x}_j)^2 + v_0 \right], \quad (2.2)$$

where \mathbf{x}_i is a position vector of i th quark, v_0 is a mass shift parameter, and λ_i^α are the Gell-Mann matrices for color; note that $\lambda_i^\alpha \rightarrow -\tilde{\lambda}_i^\alpha$ for antiquark. The color-magnetic potential V_{CM} is

$$V_{\text{CM}} = \sum_{i < j} \sum_{\alpha=1}^8 \frac{\lambda_i^\alpha}{2} \frac{\lambda_j^\alpha}{2} \frac{\xi_\sigma}{m_i m_j} e^{-(\mathbf{x}_i - \mathbf{x}_j)^2 / \beta^2} \boldsymbol{\sigma}_i \cdot \boldsymbol{\sigma}_j. \quad (2.3)$$

Parameters in the Hamiltonian are fixed as follows. First we take standard values, $m_u = m_d = 330$ MeV and $m_{\bar{s}} = 500$ MeV, for quark masses. And as for k and β we take the same values as in Refs. [4, 5], i.e. $k = 455.1$ MeV·fm⁻² and $\beta = 0.5$ fm. The remainder ξ_σ and v_0 are so determined that the three-body calculation, done in the same manner as in Ref. [13], can reproduce $m_N = 939$ MeV and $m_\Delta = 1232$ MeV. The resultant values are $\xi_\sigma/m_u^2 = -474.9$ MeV and $v_0 = -428.3$ MeV. The parameters thus determined are assumed to be universal for all low-lying hadrons including the pentaquark.

One may wonder whether a linear confinement potential should be used instead of the harmonic oscillator potential. The latter potential, however, has been used in many previous studies, since it is easy to handle. In our present analysis, rather than the practical advantage, we point out that as long as low lying states up to $\hbar\omega \sim$ several hundreds MeV are concerned, their properties are rather insensitive to the type of the potential. For this reason, we adopt the harmonic oscillator confining potential for the first serious calculation of the five-body system. (Recently, we have applied linear-type confinement and color-magnetic potential of ordinary baryons and mesons to the pentaquark system, and have confirmed that our main conclusion of the absence of low-lying pentaquark resonances is unchanged in this more realistic calculation [12].)

The present Hamiltonian is tested by static properties of conventional baryons and mesons. Results are summarized in Table I which shows theoretical values of masses, magnetic moments and charge radii and their corresponding experimental values. It should be emphasized that the present set of interactions satisfactorily reproduces observed masses of octet and decuplet baryons and octet mesons. We also calculated absolute strengths of non-leptonic weak decay of hyperon and found that the results reproduce the observed data owing to the qq correlation taken properly and are very close to those of the previous work [13] in which a spin-spin interaction different from V_{CM} is taken. Thus, agreement of the theoretical values with the experimental values for the two- and three-quark systems is satisfactory to proceed to the five-quark system with the same Hamiltonian.

TABLE I: Static properties of conventional mesons and baryons. Squared charge radius in the last columns is defined by $\langle \sum_i Q_i r_i^2 \rangle$ in units of fm^2 , where Q_i and r_i are charge of the i th quark and distance of the i th quark from the center of mass, respectively. Magnetic moments and squared charge radii of Δ^Q states are proportional to the charge Q .

	mass		magnetic moment		sq. charge radius	
	Cal.	Exp.	Cal.	Exp.	Cal.	Exp.
	(MeV)		(nm)		(fm^2)	
p	939	939	2.7735	2.7828	$(0.60)^2$	$(0.87)^2$
n	939	939	-1.826	-1.913	-0.04	-0.12
Λ	1058	1115	-0.613	-0.613	-0.004	-
Σ^+	1119	1189	2.695	2.458	0.44	-
Σ^0	1119	1192	0.822	-	0.06	-
Σ^-	1119	1197	-1.050	-1.160	-0.31	-
Ξ^0	1221	1314	-1.466	-1.250	-0.06	-
Ξ^-	1221	1321	-0.518	-0.651	-0.28	-
Δ^Q	1232	1232	$2.843Q$	-	$0.41Q$	-
Σ^{*+}	1320	1384	3.17	-	0.52	-
Σ^{*0}	1320	1384	0.32	-	0.07	-
Σ^{*-}	1320	1384	-2.52	-	-0.38	-
Ξ^{*0}	1414	1533	0.64	-	0.12	-
Ξ^{*-}	1414	1533	-2.20	-	-0.35	-
Ω	1506	1672	-1.877	-2.02	-0.32	-
K^\pm	483	495			± 0.15	
K^0	483	495			-0.04	
π^\pm	206	140			± 0.12	
π^0	206	140			0.0	
ρ^\pm	740	770			± 0.28	
ρ^0	740	770			0.0	
ω	740	783			0.0	
ϕ^0	939	1020			0.0	
$K^{*\pm}$	839	892			± 0.29	
K^{*0}	839	892			-0.07	

III. METHOD

We solve the five-body Schrödinger equation

$$(H - E) \Psi_{J^\pi M} = 0, \quad (3.1)$$

imposing the scattering boundary condition to the NK scattering component of the total wave function $\Psi_{J^\pi M}$; here $\Psi_{J^\pi M}$ is classified with the angular momentum J , its z -component M and parity π . The NK scattering component of $\Psi_{J^\pi M}$ is expressed by

$$\begin{aligned} & \Psi_{J^\pi M}^{(NK)}(E) \\ &= \mathcal{A}_{1234} \left\{ \left[\phi_{\frac{1}{2}}^{(N)}(123) \phi_0^{(K)}(45) \right]_{\frac{1}{2}} \chi_L(\mathbf{R}_1) \right\}_{J^\pi M}, \quad (3.2) \end{aligned}$$

where the operator \mathcal{A}_{1234} antisymmetrizes particles 1–4 (u, d quarks) while particle 5 is \bar{s} . Here, $\phi_{\frac{1}{2}}^{(N)}$ and $\phi_0^{(K)}$

are the color-singlet spin $\frac{1}{2}$ and spin 0 intrinsic wave functions of N and K , respectively, and $\chi_L(\mathbf{R}_1)$ is the wave function of the NK relative motion along the coordinate \mathbf{R}_1 (cf. $c = 1$ of Fig. 1) with the angular momentum L and the center-of-mass energy $E - E_{\text{th}}$, E_{th} being the NK threshold energy (1422 MeV in the present model). The reported energy of $\Theta^+(1540)$ is slightly above the NK threshold, it is then convenient to consider the pentaquark energy E with $E - E_{\text{th}}$.

The interaction-region part of $\Psi_{J^\pi M}$ should be described with a large model space. For this purpose, we take five Jacobi-coordinate set, $c = 1 - 5$ of Fig. 1, and construct the L^2 -type basis functions, $\Phi_{J^\pi M, \alpha}^{(c)}$, for each coordinate c as follows:

$$\begin{aligned} \Phi_{J^\pi M, \alpha}^{(c)} &= \mathcal{A}_{1234} \left\{ \xi_1^{(c)}(1234, 5) \eta_{0(t)}^{(c)}(1234, 5) \right. \\ &\times \left. \left[\chi_{S(s\bar{s}\sigma)}^{(c)}(1234, 5) \psi_{L\{n\}}^{(c)}(\mathbf{r}_c, \boldsymbol{\rho}_c, \mathbf{s}_c, \mathbf{R}_c) \right]_{J^\pi M} \right\}, \quad (3.3) \end{aligned}$$

where $\xi_1^{(c)}$ is the color-singlet wave function, and $\eta_{0(t)}^{(c)}$, $\chi_{S(s\bar{s}\sigma)}^{(c)}$ and $\psi_{L\{n\}}^{(c)}$ are the isospin, spin and spatial wave functions with the total isospin $T = 0$, the total spin $S = \frac{1}{2}$ and the total orbital angular momentum L , respectively. Here we have neglected $S = \frac{3}{2}$, since it is decoupled to the $N + K$ scattering channel with $S = \frac{1}{2}$. Here, t and s, \bar{s}, σ are intermediate quantum numbers of isospin and spin coupling, respectively, and as shown in the next section the symbol $\{n\}$ specifies the radial dependence of the spatial wave functions. The suffix α in $\Phi_{J^\pi M, \alpha}^{(c)}$ specifies a set of $(t, S, s, \bar{s}, \sigma, L, \{n\})$.

The Hamiltonian is diagonalized within a model space spanned by a large number of $\Phi_{J^\pi M, \alpha}^{(c)}$, that is, $\sim 15,000$ basis functions in actual calculations. The resulting discrete eigenstates are called pseudostates, when the eigenenergies E_ν satisfy $E_\nu > E_{\text{th}}$. The pseudostates, $\{\hat{\Phi}_{J^\pi M}(E_\nu); \nu = 1 - \nu_{\text{max}}\}$, are written in terms of $\Phi_{J^\pi M, \alpha}^{(c)}$ as

$$\hat{\Phi}_{J^\pi M}(E_\nu) = \sum_{c, \alpha} A_{J, \alpha}^{(c)}(E_\nu) \Phi_{J^\pi M, \alpha}^{(c)}(\mathbf{r}_c, \boldsymbol{\rho}_c, \mathbf{s}_c, \mathbf{R}_c). \quad (3.4)$$

It is possible to expand the interaction-region part of the total wave function in term of those eigenfunctions since they are considered to form a complete set for each J^π in the finite interaction region. The total wave function is then described as a superposition of the NK scattering component and the $\hat{\Phi}_{J^\pi M}(E_\nu)$:

$$\Psi_{J^\pi M}(E) = \Psi_{J^\pi M}^{(NK)}(E) + \sum_{\nu=1}^{\nu_{\text{max}}} b_\nu(E) \hat{\Phi}_{J^\pi M}(E_\nu). \quad (3.5)$$

The second term describes virtual excitations of N and K in $c = 1$ and other five-body distortions in $c = 2 - 5$ in the intermediate stage of the scattering. Unknown quantities $\chi_L(\mathbf{R}_1)$ in $\Psi_{J^\pi M}^{(NK)}(E)$ and $b_\nu(E)$ are obtained by solving Eq. (3.1) with the Kohn-type variational method [6]. Inclusion of high-lying pseudostates in the model space do

not change calculated values of the phase shift, when the energies E_ν are much larger than the NK scattering energy. Hence, only a few tens of lowest-lying pseudostates contribute to the numerical calculation. In the present calculation, the NK scattering energy should be smaller than an energy of the first spatial excited state of nucleon, i.e. the Roper resonance which is located at 675 MeV above the nucleon mass in the present model, because we consider only the NK scattering component as an open channel. The condition for our calculation to be valid is then $E - E_{\text{th}} < 675$ MeV. For simplicity, we also ignore the NK^* channel, since we found that inclusion of the channel little affects the conclusion of the present work. We also analyzed the $J^\pi = \frac{1}{2}^+$ resonance of $S = \frac{3}{2}$ and $L = 1$. It is not coupled to the NK scattering channel with $S = \frac{1}{2}$ but to the NK^* channel. Therefore, it will have a small width, if it appears. However, we confirmed that this is not realized at $E - E_{\text{th}} < 675$ MeV. These points will be discussed in the forthcoming paper.

IV. BASIS FUNCTIONS

Explicit definitions of the color wave functions $\xi_1^{(c)}(1234, 5)$ are as follows:

$$\begin{aligned}\xi_1^{(1)} &= [(123)_1(45)_1]_1, & \xi_1^{(2)} &= [(12)_3(45)_1]_3 3]_1, \\ \xi_1^{(3)} &= [(12)_3[(45)_1 3]_3]_1, & \xi_1^{(4)} &= [(12)_3(34)_3]_3 5]_1, \\ \xi_1^{(5)} &= [(12)_3[(34)_3 5]_3]_1\end{aligned}\quad (4.1)$$

with obvious notation; note that $\xi_1^{(1)} = \xi_1^{(2)} = \xi_1^{(3)}$ and $\xi_1^{(4)} = \xi_1^{(5)}$ due to the recombination of colors. The $\xi_1^{(c)}$ are connected for $c = 4, 5$ and molecular for other c , since there is no color-singlet cluster in the case of $c = 4, 5$.

The isospin wave functions $\eta_{0(t)}^{(c)}(1234, 5)$ with the total isospin 0 and the intermediate isospin $t (= 0, 1)$ are described as

$$\begin{aligned}\eta_{0(t)}^{(1)} &= [(12)_t 3]_{\frac{1}{2}} (45)_{\frac{1}{2}}]_0, & \eta_{0(t)}^{(2)} &= [(12)_t (45)_{\frac{1}{2}}]_{\frac{1}{2}} 3]_0, \\ \eta_{0(t)}^{(3)} &= [(12)_t [(45)_{\frac{1}{2}} 3]_t]_0, & \eta_{0(t)}^{(4)} &= [(12)_t (34)_t]_0 5]_0, \\ \eta_{0(t)}^{(5)} &= [(12)_t [(34)_t 5]_t]_0.\end{aligned}\quad (4.2)$$

The spin functions $\chi_{\frac{1}{2}(s\bar{s}\sigma)}^{(c)}(1234, 5)$ are also described as

$$\begin{aligned}\chi_{\frac{1}{2}(s\bar{s}\sigma)}^{(1)} &= [(12)_s 3]_\sigma (45)_{\bar{s}}]_{\frac{1}{2}}, & \chi_{\frac{1}{2}(s\bar{s}\sigma)}^{(2)} &= [(12)_s (45)_{\bar{s}}]_\sigma 3]_{\frac{1}{2}}, \\ \chi_{\frac{1}{2}(s\bar{s}\sigma)}^{(3)} &= [(12)_s [(45)_{\bar{s}} 3]_\sigma]_{\frac{1}{2}}, & \chi_{\frac{1}{2}(s\bar{s}\sigma)}^{(4)} &= [(12)_s (34)_{\bar{s}}]_\sigma 5]_{\frac{1}{2}}, \\ \chi_{\frac{1}{2}(s\bar{s}\sigma)}^{(5)} &= [(12)_s [(34)_{\bar{s}} 5]_\sigma]_{\frac{1}{2}}.\end{aligned}\quad (4.3)$$

Finally, the spatial wave function $\psi_{L\{n\}}^{(c)}(\mathbf{r}_c, \boldsymbol{\rho}_c, \mathbf{s}_c, \mathbf{R}_c)$ with the total orbital angular momentum L , where $L = 0$ for $J^\pi = \frac{1}{2}^-$ and $L = 1$ for $J^\pi = \frac{1}{2}^+$, is assumed as

$$\begin{aligned}\psi_{L\{n\}}^{(c)}(\mathbf{r}_c, \boldsymbol{\rho}_c, \mathbf{s}_c, \mathbf{R}_c) \\ = \phi_{n_r 00}^{(c)}(\mathbf{r}_c) \phi_{n_\rho 00}^{(c)}(\boldsymbol{\rho}_c) \phi_{n_s 00}^{(c)}(\mathbf{S}_c) \phi_{n_R L_c M}^{(c)}(\mathbf{R}_c).\end{aligned}\quad (4.4)$$

Here we have set the orbital angular momenta $\{L_{x_c}\}$ associated with coordinates $x_c = \mathbf{r}_c, \boldsymbol{\rho}_c, \mathbf{s}_c$ to be zero and the angular momentum L_c associated with \mathbf{R}_c to be L ; as shown below, however, this does not mean that the angular momentum space is small. The set $\{n\} = \{n_r, n_\rho, n_s, n_R\}$ specifies the radial dependence of the four basis functions $\phi^{(c)}$. In GEM, the functions $\phi_{n_R L_c M}(\mathbf{R})$ are written as

$$\phi_{n_R L_c M}(\mathbf{R}) = R^{L_c} e^{-(R/\bar{R}_{n_R})^2} Y_{L_c M}(\hat{\mathbf{R}}) \quad (4.5)$$

with the Gaussian ranges taken in geometric progression,

$$\bar{R}_{n_R} = \bar{R}_1 a^{n_R - 1} \quad (n_R = 1 - n_R^{\max}) \quad (4.6)$$

with $a = (\bar{R}_{n_R^{\max}}/\bar{R}_1)^{1/(n_R^{\max} - 1)}$. Here, n_R^{\max} , \bar{R}_1 and $\bar{R}_{n_R^{\max}}$ depend upon c , isospin and spin taken, but the explicit dependence is suppressed for simplicity of notation. The same procedure is taken also for $\phi_{n_r 00}^{(c)}(\mathbf{r}_c)$, $\phi_{n_\rho 00}^{(c)}(\boldsymbol{\rho}_c)$ and $\phi_{n_s 00}^{(c)}(\mathbf{S}_c)$.

In GEM, the model space is constructed by superposing the Gaussian basis functions (4.4) over all c from 1 to 5. This superposition is inevitable to describe few-body wave functions accurately, particularly when the wave functions have properties of strong short-range correlations and/or long-range tails; many examples are shown in [8]. As a consequence of the superposition, furthermore, the fact that $\{L_{x_c}\} = 0$ in (4.4) does not mean that the angular momentum space is small. As a simple example, let us consider a base with $\{L_{x_c}, L_c\} = 0$, $e^{-(r_c/\bar{r})^2 - (\rho_c/\bar{\rho})^2 - (S_c/\bar{S})^2 - (R_c/\bar{R})^2}$. The base can be rewritten in terms of c' , i.e. $\mathbf{r}_{c'}, \boldsymbol{\rho}_{c'}, \mathbf{S}_{c'}, \mathbf{R}_{c'}$. The transformed form contains many terms with $\{L_{x_{c'}}, L_{c'}\} \neq 0$. Thus, the five-body eigenfunctions $\hat{\Phi}_{J^\pi M}(E_\nu)$ given by the superposition can cover an angular momentum space large enough to derive the phase shifts accurately.

The antisymmetrization between quarks 1 – 4 requires $s + t = \text{even}$ for $c = 1 - 3$ and $s + t = \bar{s} + t = \text{even}$ for $c = 4, 5$. For $c = 1 - 3$, $\bar{s} = 0$ is taken to omit the K^* component. The diquark model proposed for $J^\pi = \frac{1}{2}^+$ in Ref. [14] is included in our model space as a configuration of $c = 4$ with $t = s = \bar{s} = \sigma = 0$ and $L = 1$, though the diquark is treated as a boson in the model but not in the present approach.

The calculated phase shifts are converged with $n_r^{\max}, n_\rho^{\max}, n_s^{\max} = 5$ or 6 for $c = 1 - 5$ and $n_R^{\max} = 12$ for $c = 1$ and 6 for other c . Minimum and maximum ranges of the bases are, respectively, 0.2 fm and 4.0 fm for coordinate R_1 and ~ 0.2 fm and ~ 2.0 fm for other coordinates. Eventually, the model space is constructed by $\sim 15,000$ basis functions.

It is worth noting that the connected configuration of $c = 4, 5$ has a non-negligible overlap with the molecular configuration of $c = 1 - 3$ when they are localized in a small space, and in general the overlap is enhanced by the antisymmetrization \mathcal{A}_{1234} . An extreme case is the $(0s)^5 J^\pi = \frac{1}{2}^-$ shell-model configuration in which the center-of-mass motion is excluded. The configuration is

equivalent to not only a molecular configuration

$$\mathcal{A}_{1234}\{\xi_1^{(1)}\eta_{0(0)}^{(1)}\chi_{\frac{1}{2}(00\frac{1}{2})}^{(1)}e^{-\frac{r_1^2}{4b^2}-\frac{\rho_1^2}{3b^2}-\frac{3R_1^2}{5b^2}-\frac{s_1^2}{4b^2}}\} \quad (4.7)$$

but also to an connected configuration

$$\mathcal{A}_{1234}\{\xi_1^{(4)}\eta_{0(1)}^{(4)}\chi_{\frac{1}{2}(111)}^{(4)}e^{-\frac{r_4^2}{4b^2}-\frac{\rho_4^2}{4b^2}-\frac{R_4^2}{2b^2}-\frac{2s_4^2}{5b^2}}\}, \quad (4.8)$$

where $b = \sqrt{\hbar/m_u\omega} = 0.63$ fm and $\hbar\omega = (5\hbar^2k/3m_u)^{\frac{1}{2}} = 300$ MeV. Thus, the connected and the molecular configuration has 100% overlap. The $(0s)^5$ wave function is obtained as an eigenstate of the approximate Hamiltonian in which $m_s = m_u$ and $V_{\text{CM}} = 0$ are taken and the color factor $\sum_{\alpha}\lambda_i^{\alpha}\lambda_j^{\alpha}$ is replaced by its average value $-4/3$. The expectation value of the full Hamiltonian by the $(0s)^5$ $J^{\pi} = \frac{1}{2}^{-}$ configuration is 503 MeV above the NK threshold. The $(0s)^5$ configuration is not an eigenstate of the full Hamiltonian and has a large overlap with the NK scattering configuration, so it is changed into non-resonant continuum states, as shown later, when the Schrödinger equation is solved with the NK scattering component.

V. RESULTS

Firstly, we calculate the NK elastic scattering phase shifts for $J^{\pi} = \frac{1}{2}^{-}$ and $\frac{1}{2}^{+}$, by omitting the pseudostate terms in (3.5). In this calculation, N and K behave as inert particles. The resulting phase shifts are shown in Fig. 2 as dash-dotted lines. There appears no resonance in the entire energy region.

Next, we do the full-fledged calculation including the pseudostate terms in (3.5). Calculated phase shifts are shown as solid lines. Up to the energy $E \sim 300$ MeV, the calculated phase shifts of $J^{\pi} = \frac{1}{2}^{-}$ agree qualitatively well with the experimental data [15, 16] as well as with the previous quark model estimations [17].

No resonance is seen in the energy region 0 – 500 MeV above the NK threshold (1.4 – 1.9 GeV in mass), that is, in the reported energy region of $\Theta^{+}(1540)$. One does see two resonances around 530 MeV; one is a sharp $J^{\pi} = \frac{1}{2}^{-}$ resonance with a width of $\Gamma = 0.12$ MeV located at $E - E_{\text{th}} = 540$ MeV and the other is a broad $\frac{1}{2}^{+}$ resonance at ~ 520 MeV with $\Gamma \sim 110$ MeV. It should be noted here that our result on the absence of the low-lying pentaquark resonance is consistent with some recent lattice QCD results in Refs. [19, 20, 21], in which, in fact, no pentaquark resonance is observed below about 300 MeV with respect to the $N + K$ threshold.

We investigate properties of the sharp $J^{\pi} = \frac{1}{2}^{-}$ resonance by using Eq. (3.5) in its second term. In the interaction region which we are interested in, the amplitude of the second (pseudostate) term is much larger than that of the first (scattering-channel) one. Thus, the sharp resonance is not a molecular state of N and K in their ground states. Figure 3 shows the one-body density of the resonance state in its u, d quark component

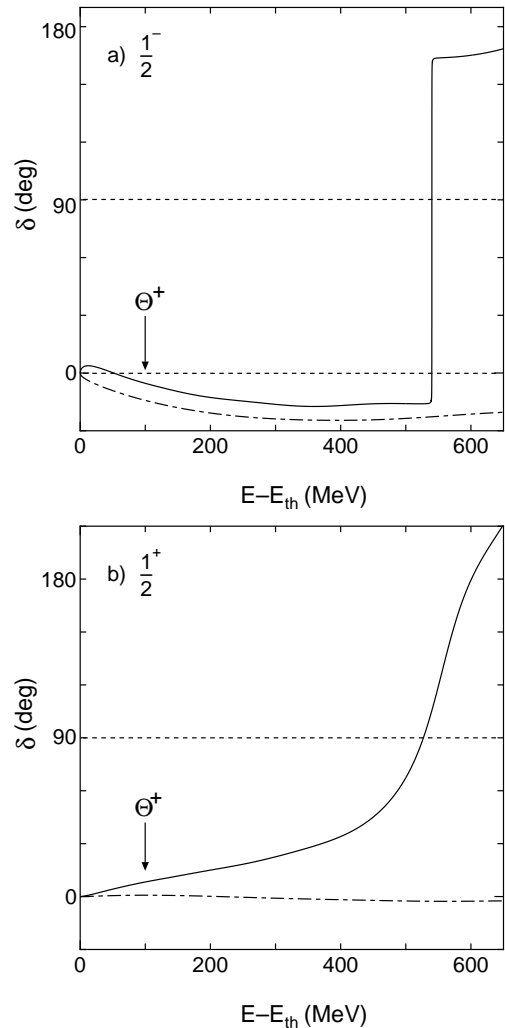


FIG. 2: Calculated phase shifts for a) $J^{\pi} = \frac{1}{2}^{-}$ and b) $J^{\pi} = \frac{1}{2}^{+}$ states. The solid lines are given by the full-fledged calculation, while the dash-dotted lines are by the approximate calculation with the elastic NK channel alone (see (3.5)). Energies are measured from the NK threshold. The arrow indicates the energy of $\Theta^{+}(1540)$ in $E - E_{\text{th}}$.

and \bar{s} quark one. One can see from the density that a \bar{s} quark is localized near the center and surrounded by u, d quarks which are totally antisymmetrized but spatially symmetrized. The density of u, d quarks is found to be very broad compared with that of the $(0s)^5$ state. This indicates that u, d quarks are not in $(0s)$ shell but in higher shells. Actually, the overlap of the second term of Eq. (3.5) with the $(0s)^5$ configuration is only 2 %. Furthermore, the one-body r.m.s. radius measured from the center of mass is 1.10 fm for u, d quarks and 0.72 fm for \bar{s} quark, while the corresponding radius is 0.69 fm for the $(0s)^5$ configuration. Thus, the structure of the sharp resonance is quite far from the $(0s)^5$ configuration, although the expectation energy of the $(0s)^5$ configuration is rather close to the resonance energy. As for the broad $J^{\pi} = \frac{1}{2}^{+}$ resonance, the one-body density cannot

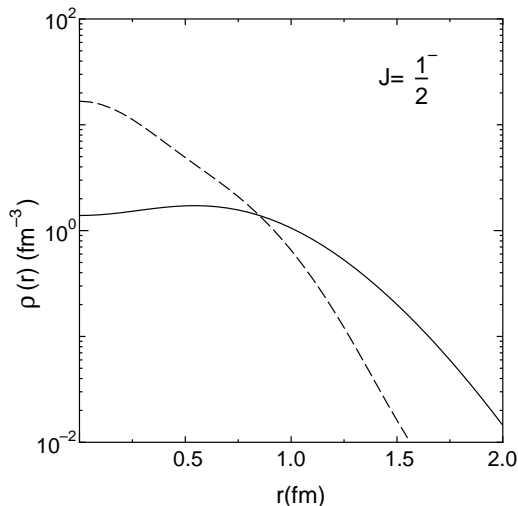


FIG. 3: One-body density $\rho(r)$ of the $J^\pi = \frac{1}{2}^-$ resonance at $E - E_{\text{th}} = 540$ MeV as a function of r that denotes the distance of a quark with respect to the center of mass. The density of u, d quark is given by the solid line while that of \bar{s} quark is by the dashed line. $\rho(r)$ is normalized as $\int_0^\infty \rho(r)r^2 dr = 1$.

be estimated meaningfully, since the second term are not dominant in Eq. (3.5).

In general neither pure connected nor pure molecular resonance exists, since any connected and molecular configurations are non-orthogonal to each other due to the antisymmetrization. Nevertheless, we can determine whether the two resonances are connected or molecular in their main components. The phase shifts shown above are not changed significantly when the connected components ($c=4, 5$) are omitted from the basis (3.3); for example, the resonance energy goes up only by 6 MeV for the $J^\pi = \frac{1}{2}^-$ state and by 15 MeV for the $J^\pi = \frac{1}{2}^+$ state. In contrast, when the molecular components ($c = 1 - 3$) are omitted, the $J^\pi = \frac{1}{2}^-$ resonance disappears from the entire energy region and the $J^\pi = \frac{1}{2}^+$ resonance is shifted upward by 130 MeV. This result means that the two resonances are molecular in their dominant components. Thus, as for both the resonances the five-body configurations in the interaction region, represented by the second term of (3.5), are mainly molecular, that is, they are composed of color-singlet but spatially distorted (excited) $(qqq)_1$ and $(q\bar{q})_1$ clusters. The reason why the five-body system is mainly molecular at energies concerned in this work is as follows. Since the $(q\bar{q})_1$ correlation is twice as attractive as the $(qq)_3$ one, in general the molecular configuration with one qq pair and one $q\bar{q}$ pair (cf. $c = 1 - 3$ in Fig. 1) obtain an energy gain larger than the connected configuration with two qq pairs (cf. $c = 4, 5$) does. Thus, the molecular five-body configuration in which the qq and $q\bar{q}$ correlations work most effectively appears as low-lying states of the pentaquark system. For the two resonance states $(qqq)_1$ and $(q\bar{q})_1$ clusters are spatially distorted to a large extent, while for non-resonance states the distortion is rather weak.

Exotic resonances might appear at energies much higher than the two molecular resonances do, but it is out of scope of this paper since some inelastic scattering channels are opened there.

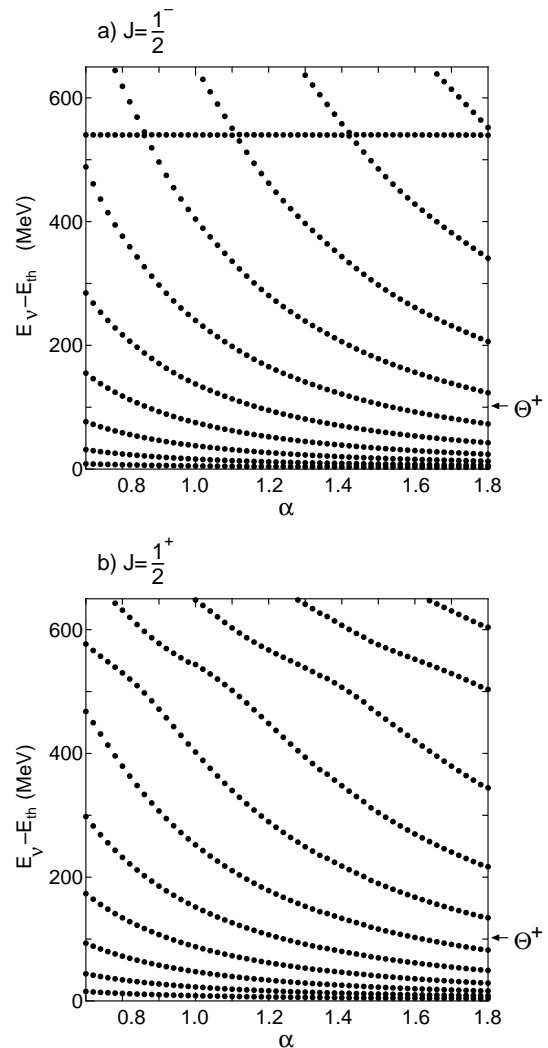


FIG. 4: The stabilization plots of the eigenenergies E_ν of the pseudostates against the scaling factor α for a) $J^\pi = \frac{1}{2}^-$ and b) $J^\pi = \frac{1}{2}^+$. Here, the Gaussian ranges \bar{R}_{n_R} associated with the coordinate \mathbf{R}_1 is scaled as $\bar{R}_{n_R} \rightarrow \alpha \bar{R}_{n_R}$ with $0.7 \leq \alpha \leq 1.8$; The arrow indicates the energy of $\Theta^+(1540)$ in $E_\nu - E_{\text{th}}$.

All the nonrelativistic quark-model calculations done so far for the pentaquark system use the bound-state approximation in which the NK scattering component does not exist asymptotically. Therefore, it is of interest to compare the scattering phase shifts with the eigenenergies (E_ν) of the pseudostates as a result of the bound-state approximation. In general, in the case of a sharp resonance, there is an eigenenergy E_ν of the Hamiltonian that is close to the resonance energy, and the energy E_ν is stable with respect to scaling the ranges of the basis functions associated with \mathbf{R}_1 the coordinate of the NK scattering, since the asymptotic amplitude of the

sharp resonance is relatively much smaller than the internal amplitude. In contrast, other pseudostates have eigenenergies E_ν which decrease monotonously with the increasing the ranges, because so does the kinetic energy associated with \mathbf{R}_1 .

These characteristics are really seen in Fig. 4 that shows stabilization plots of E_ν with respect to the scaling $R_{n_R} \rightarrow \alpha R_{n_R}$; the parameter α corresponds to the volume size in the lattice calculation. This plotting to investigate resonances is called the real-scaling (stabilization) method [18]. In Fig. 4a for $J^\pi = \frac{1}{2}^-$, all pseudostates except one are unstable in the sense that they decrease toward the NK threshold. Thus, those pseudostates are regarded as a discrete representation of the non-resonant continuum spectrum. The stable (horizontal) line at $E_\nu = 540$ MeV precisely corresponds to the sharp resonance at 540 MeV in Fig. 2a. The horizontal line and the nearby unstable lines do not cross each other because of repulsive forces working between them, though it is not precisely plotted. This is called the avoiding crossing. One can roughly estimate the width of the resonance from the behavior of the avoiding crossing with the aid of Eq. (4) of Ref. [18]. In the present case, the estimated width is of order 0.1 MeV and consistent with the value obtained from the phase shift. On the other hand, the $J^\pi = \frac{1}{2}^+$ resonance at ~ 520 MeV with $\Gamma \sim 110$ MeV in Fig. 2b is too broad to be identified as a resonance from the stabilization plot of Fig. 4b, though one sees a tendency of plateaus around 500 – 600 MeV. Therefore, without the scattering calculation it is difficult to discriminate a broad resonance from non-resonance states.

In summary, we solved the five-quark scattering problem by applying GEM [8] and the Kohn-type variational method [6] to the large model space including the NK scattering component. We adopted the standard non-relativistic quark model of Isgur-Karl which satisfactorily reproduces experimental values of the two- and three-quark systems. The resultant NK scattering phase shift showed no resonance in the reported energy region of $\Theta^+(1540)$; this is the most important result of the present paper. At energies much higher (by ~ 400 MeV) than the $\Theta^+(1540)$ energy, we did find a broad $J^\pi = \frac{1}{2}^+$ resonance with $\Gamma \sim 110$ MeV at ~ 520 MeV above the NK threshold and a sharp $J^\pi = \frac{1}{2}^-$ resonance with $\Gamma = 0.12$ MeV at 540 MeV. In the present model Hamiltonian, since the $J^\pi = \frac{1}{2}^+$ and $\frac{3}{2}^+$ states are degenerate to each other, there exists a broad $J^\pi = \frac{3}{2}^+$ resonance with the same

energy and width as the $J^\pi = \frac{1}{2}^+$ resonance.

We have done the same calculation for other Hamiltonian proposed in [13] that also reproduces the observed properties of the ordinary hadrons and mesons with the same quality of agreement as in Section II. The result was qualitatively the same as in this paper; in particular resonances are absent in the low energy region up to 500 MeV from the NK threshold. The locations and the widths of the resonances at higher energies, however, depend on the details of the model hamiltonian.

The resonance states are mainly composed of color-singlet $(qqq)_1$ and $(q\bar{q})_1$ clusters which are distorted (excited) to a large extent. Thus, these are molecular resonances. The $(q\bar{q})_1$ correlation is twice as attractive as the $(qq)_3$ one, so low-lying states, no matter whether the widths are small or not, are dominated by molecular configurations. Thus, even if a resonance with a small width is measured, the fact that the width is small does not necessarily mean that the resonance is connected. The sharp $J^\pi = \frac{1}{2}^-$ resonance has a quite different structure from the $(0s)^5$ configuration. In the resonance, \bar{s} quark is located near the center and surrounded by u, d quarks which are spatially symmetrized.

Finally, we tested the reliability of the bound-state approximation with the real scaling method. Essentially the same approximation is used in the lattice calculation. We found, by comparing Fig. 4 with Fig. 2, that the approximation surely works for a sharp resonance with a width of order 0.1 MeV, but not for a broad resonance with a width of order 100 MeV and that most of the states obtained by the approximation melt into non-resonant continuum states when the NK scattering channel is included accurately. It should be noted that our model calculation with the NK scattering channel clarifies the mechanism of the disappearance of low-lying pentaquark resonance, which cannot be shown even by lattice QCD. Further analyses including NK^* scattering channel will be reported in a forthcoming paper, together with results for other (T, J^π) states.

The authors would like to thank Prof. M. Oka, Prof. H. Suganuma, Prof. M. Ohbu and Prof. M. Tanifuji for helpful discussions. This work has been supported in part by the Grant-in-Aid for Scientific Research (14540271) of Monbukagakushou of Japan and by the Nara Women's University Intramural Grant for Project Research (E.H.). The numerical calculations were done on FUJITSU VPP5000 at JAERI.

-
- [1] LEPS Collaboration, T. Nakano *et al.*, Phys. Rev. Lett. **91**, 012002 (2003).
 - [2] For a recent review, for instance, see A. Dzierba *et al.*, hep-ex/0412077.
 - [3] For a review, for instance, M. Oka, Prog. Theor. Phys. **112**, 1 (2004) and references therein.
 - [4] N. Isgur and G. Karl, Phys. Rev. D **20**, 1191 (1971).
 - [5] J. Weinstein and N. Isgur, Phys. Rev. D **27**, 588 (1983).
 - [6] M. Kamimura, Prog. Theor. Phys. Suppl. **62**, 236 (1977); also see Section 8 of [8].
 - [7] M. Oka and K. Yazaki, Prog. Theor. Phys. **66**, 556, 572 (1981).
 - [8] E. Hiyama, Y. Kino and M. Kamimura, Prog. Part. Nucl. Phys. **51**, 223 (2003).
 - [9] S. Eidelman *et al.*, Phys. Lett. B **592**, 1 (2004).
 - [10] Y. Kino, M. Kamimura and H. Kudo, in Proc. Inter.

- Conf. on Low Energy Antiproton Physics, Yokohama, 2003 (Inst. Meth. Phys. Res. B **214** (2004) 84).
- [11] M. Hori *et al.*, Phys. Rev. Lett. **91**, 123401 (2003).
 - [12] E. Hiyama *et al.*, in preparation.
 - [13] E. Hiyama, K. Suzuki, H. Toki and M. Kamimura, Prog. Theor. Phys. **112**, 99 (2004).
 - [14] R. Jaffe and F. Wilczek, Phys. Rev. Lett. **91**, 232003, (2003).
 - [15] K. Hashimoto, Phys. Rev. C**29**, 1377 (1984).
 - [16] J.S. Hyslop, R.A. Arndt, L.D. Roper, and R.L. Workman, Phys. Rev. D**46**, 961 (1992).
 - [17] I. Bender *et. al.*, Nucl. Phys. **A725**, 171 (1984)
 - [18] J. Simons, J. Chem. Phys. **75**, 2465 (1981).
 - [19] N. Mathur *et al.*. Phys. Rev. D **70**, 074508 (2004).
 - [20] N. Ishii, T. Doi, H. Iida, M. Oka, F. Okihara and H. Suganuma, Phys. Rev. D**71**, 034001 (2005).
 - [21] T. T. Takahashi, T. Umeda, T. Onogi and T. Kunihiro, Phys. Rev. D**71**, 114509 (2005).